Uranium-series comminution ages of continental sediments: Case study of a Pleistocene alluvial fan

Victoria E. Lee [a, 1 *], Donald J. DePaolo [a,b], John N. Christensen [b]

[a] *Dept. of Earth & Planetary Science, University of California, Berkeley, 307 McCone Hall, Berkeley, CA 94720-4767 USA*
[b] *Earth Sciences Division, Lawrence Berkeley National Laboratory, 1 Cyclotron Rd., MS 70A4418, Berkeley, CA 94720 USA*

* Corresponding author Tel.: +44 (0)1865 272969; Fax: +44 (0)1865 272072
[1] current address: Dept. of Earth Sciences, University of Oxford, Parks Road, Oxford, OX1 3PR, United Kingdom
email addresses: victoria.lee@earth.ox.ac.uk (V.E. Lee), depaolo@eps.berkeley.edu (D.J. DePaolo), JNChristensen@lbl.gov (J.N. Christensen)

Abstract

Obtaining quantitative information about the timescales associated with sediment transport, storage, and deposition in continental settings is important but challenging. The uranium-series comminution age method potentially provides a universal approach for direct dating of Quaternary detrital sediments, and can also provide estimates of the sediment transport and storage timescales. (The word "comminution" means "to reduce to powder," reflecting the start of the comminution age clock as reduction of lithic parent material below a critical grain size threshold of ~50 μm.) To test the comminution age method as a means to date continental sediments, we applied the method to drill-core samples of the glacially-derived Kings River Fan alluvial deposits in central California. Sediments from the 45 m core have independently-estimated depositional ages of up to ~800 ka, based on paleomagnetism and correlations to nearby dated sediments. We characterized sequentially-leached core samples (both bulk sediment and grain size separates) for U, Nd, and Sr isotopes, grain size, surface texture, and mineralogy. In accordance with the comminution age model, where ^{234}U is partially lost from small (<50 μm) sediment grains due to alpha recoil, we found that ($^{234}U/^{238}U$) activity ratios generally decrease with age, depth, and specific surface area, with depletions of up to 9% relative to radioactive equilibrium. The resulting calculated comminution ages are reasonable, although they do not exactly match age estimates from previous studies and also depend on assumptions about ^{234}U loss rates. The results indicate that the method may be a significant addition to the sparse set of available tools for dating detrital continental sediments, following further refinement. Improving the accuracy of the method requires more advanced models or measurements for both the recoil loss factor f_α and weathering effects. We discuss several independent methods for obtaining f_α on individual samples that may be useful for future studies.

Keywords: isotope geochemistry; U-series isotopes; sediment; geochronology; Quaternary; Sierra Nevada

1. Introduction

The lifetimes of clastic sediment particles in continental settings – from initial formation by weathering and erosion, to transport, storage, deposition, and lithification – both reflect and control the nature of geologic processes in the Earth's surface environment. Among the interrelated areas of interest in which the timing, rates, and durations of sedimentary processes play a key role are: understanding mechanisms of landscape evolution (Dietrich et al., 1982; Dietrich et al. 2003); modulating elemental cycles by controlling the residence time of sediments in natural reservoirs such as floodplains (Dunne et al., 1998, and refs. therein); formation and interpretation of depositional records of paleoclimate and tectonic activity (e.g., Phillips et al., 1997; Last and Smol, 2001; Molnar, 2004); influencing the long-term, erosion-driven drawdown of atmospheric CO_2 by silicate weathering (Raymo and Ruddiman, 1992); and determining sediment flux to the oceans (Hay, 1998; Syvitski et al., 2003).

Although quantifying the timescales of sedimentary cycling is important, obtaining this information is difficult, especially over geologic timescales where direct observation is not possible. Uranium-series isotopes may be helpful in this regard. The isotopic fractionation between various nuclides of the uranium-series decay chains can be used to provide information about sediment history, behavior, and weathering over time periods up to ~10^6 yrs (e.g., Osmond and Ivanovich, 1992; Vigier et al., 2001; Chabaux et al., 2003; Granet et al., 2007; Dosseto et al., 2008). In particular, the uranium-series comminution age method (DePaolo et al., 2006) may provide a way to directly date detrital Quaternary sediments and yield information about the timescales of sedimentary processes (Figure 1). (The word "comminution" means "to reduce to powder," and refers to the start of the U isotope age clock when bedrock has been reduced by weathering and erosion below a critical grain size threshold to form silt- and clay-sized detrital particles.)

This study evaluates whether the comminution age method, previously applied to well-sorted marine sediments (DePaolo et al., 2006), has applicability to the more challenging case of poorly-sorted continental sediments. Continental sediments are often not suitable for dating by other methods (e.g., cosmogenic radionuclide dating, biostratigraphy, and chemostratigraphy), and may have uranium-hosting nondetrital phases that could perturb the comminution age method as well. We measured uranium isotopes and other characteristics of alluvial fan sediments having independently-estimated depositional ages. Sample pretreatment methods for sequential leaching and sieving were also developed, applied, and evaluated.

2. Comminution age method

The comminution age model (DePaolo et al., 2006) is based on the loss of ^{234}U from a sediment particle due to alpha recoil following decay of the ^{238}U parent (Kigoshi, 1971). In the ^{238}U decay series, this recoil loss occurs via the alpha decay of ^{238}U to an intermediate short-lived ^{234}Th, which then rapidly undergoes beta decay (without significant recoil) to ^{234}U. The ^{234}Th precursor to ^{234}U is recoiled an average distance of ~34 nm in typical silicate minerals (Sun and Semkow, 1998; Maher et al., 2006), a distance that varies only a few nm due to straggling and variations in the compositions (density) of common crustal minerals (Hashimoto et al., 1985). For grains smaller than a threshold diameter of ~50 μm, recoil loss of ^{234}U results in a measurable decrease in ($^{234}U/^{238}U$). (Parentheses denote the activity ratio, the $^{234}U/^{238}U$ isotope ratio normalized by the $^{234}U/^{238}U$ ratio of a standard in secular, or radioactive, equilibrium.) Therefore, if alpha recoil is the only process that separates ^{234}U from ^{238}U, the measured ($^{234}U/^{238}U$) ratio of a sediment grain, A_{meas}, is a function of four parameters related by the following expression:

$$A_{meas} = (1 - f_\alpha) + [A_0 - (1 - f_\alpha)]e^{-\lambda_{234} t_{comm}} \qquad (1)$$

where t_{comm} is the amount of time elapsed since the grain became smaller than the threshold size, referred to as the *comminution age*, f_α is the fraction of ^{238}U decays that result in direct recoil loss of the ^{234}U daughter (f_α thus should be correlated with the grain surface area and size), λ_{234} is the ^{234}U decay constant (λ_{234} = 2.82629 x 10^{-6} yr^{-1}), and A_0 is the ($^{234}U/^{238}U$) of the parent material from which the sediment grains are derived. A_o is commonly assumed to be the secular equilibrium value ($^{234}U/^{238}U$) = 1 for nonporous, crystalline rocks. This method of determining a comminution age is limited to ages less than ~1 Ma, since A_{meas} will reach a grain-size-dependent steady state value after about four half lives of ^{234}U.

The uranium-series comminution age dating method differs from many existing methods for dating continental detrital sediment deposits in that it is a direct dating method with minimal restrictions on material requirements, and the comminution age contains information about not just depositional age, but also transport + storage timescales. The only theoretical requirement for comminution age dating, a uranium-bearing fine-grained sediment component, is easily fulfilled for most lithologic compositions and deposit types. Other dating methods are generally limited by requirements for specific types and/or quantities of material that may not be universally present in the sediment. Examples include nondetrital materials such as organic matter (^{14}C dating), fossils (biostratigraphy), volcanic marker units (K-Ar and Ar-Ar dating), and select authigenic phases such as carbonate (U-series and stable isotope dating), as well as detrital matter: large quantities of quartz (cosmogenic radionuclide (CRN) techniques, e.g., $^{26}Al/^{10}Be$ burial dating and ^{10}Be exposure dating (Gosse and Phillips, 2001)), and quartz or feldspar (optically stimulated luminescence (OSL) dating (Aitken, 1998)). Nondetrital dating methods generally yield only the depositional age. Detrital sediment ages obtained by CRN and OSL dating methods should provide complementary information to comminution ages, taking into account fundamental differences in what age is being recorded in the sediments (given the different underlying physico-chemical mechanisms that produce age signals for each method), as well as potential dissimilarities in the histories of the different grain size or mineral fractions being dated.

3. Study area: Kings River Fan

There are several reasons why the Kings River Fan (KRF) was selected as a study area to test the comminution age method on continental sediments. First, the expected comminution ages can be figured out – there are independent constraints on depositional age, sediment transport + storage times can be treated as negligible, and sediment production by glacial erosion implies rapid particle formation and thus a well-defined start to the comminution age clock. Second, the parent lithology is largely crystalline, allowing the assumption of A_0 = 1 to hold. Third, the potential complicating effects of subaerial weathering on U isotope behavior are minimal for the samples studied.

The Kings River Fan is a large (3150 km^2) alluvial fan located off the western slope of the Sierra Nevada in central California (Figure 2). Sediment in this fan derives from a catchment with an area of 4400 km^2 (Weissmann et al., 2005), which is underlain almost entirely by crystalline rocks of the Sierra Nevada batholith and related pre-intrusive metamorphic rocks. Approximately the upper half of the basin was covered with ice during peak Pleistocene glaciations (Wahrhaftig and Birman, 1965). In this glaciated area, where erosion was probably most rapid, the bedrock is predominantly granitic.

Samples used in this study are from a 45 m-long sediment core taken near the present-day fan apex (36°42’58” N, 119°38’53” W). This is designated as Core B5 in Burow et al. (1999) and Weissmann et al. (2002). Three depositional facies can be identified: channel deposits, overbank deposits, and moderately mature paleosols (Figure 3a), all composed of glacial flour and coarser sediment originating from Pleistocene glaciations in the Sierra Nevada (Weissmann et al., 2002, and refs. therein).

Inferred depositional ages of the sediments in the KRF core as a function of depth are shown in Figure 3b. The deepest samples have the most well-constrained ages: paleomagnetic measurements on the core samples indicate that the Matuyama-Brunhes magnetic reversal (780 ka) occurs near 41 m depth (Weissmann et al., 2002). Additional age information is obtained by correlation to type sections described in Marchant and Allwardt (1981) using the age inferences of Lettis (1988), which comprise the commonly-accepted chronology for the fan deposits of the eastern San Joaquin Valley. The age-depth model includes temporal hiatuses between major depositional units, corresponding to an episodic model of fan formation in which Sierra Nevada glaciations caused aggradation of glacigenic sediment, and interglacial times correspond to negligibly small deposition rates and the resultant formation of capping soils (Marchand, 1977;

Huntington, 1980; Marchand and Allwardt, 1981; Lettis,1988; Weissmann et al., 2002). The Upper-Middle Riverbank Formation is usually associated with marine isotope stages (MIS) 6 and 8 (ca. 130 – 280 ka), the Upper Turlock Formation with MIS 16 and/or 18 (ca. 650 – 740 ka), and the Lower Turlock Formation with MIS 20. The age constraints on the Turlock Lake units in particular rely on the 615 ka age of the Friant Pumice marker bed (Janda, 1965; Lettis 1988), but more recent dating of constituent pumice clasts produce ages that vary widely, so the Friant Pumice unit may not be as useful for chronostratigraphic control as originally thought (Sarna-Wojcicki et al., 2000). Thus, there is uncertainty in the detailed age-depth profile of the KRF deposits, but we believe the presence of the Matuyama-Brunhes magnetic reversal is a reliable indication that the core sediments at 40-45 m depth have ages near 800 kyr. It should also be noted that the overbank and channel facies have undergone minimal subaerial weathering (Weissmann et al., 2002).

As a starting point in the interpretation of our data, we assume that the comminution ages of the fine-grained Kings River Fan sediments are equal to the inferred depositional ages based on the literature-derived chronostratigraphic model for eastern San Joaquin Valley deposits (Figure 3b). The assumption of negligible transport and storage time is reasonable, given that large quantities of meltwater during glacial retreats would have provided an efficient means of sediment transport. Indeed, the Kings River Fan paleochannel was considerably wider (~625 m wide) with a straighter planform than the present-day channel (Weissman et al., 2002), suggesting a past river system with large sediment transport capacity. Aerial views of the Kings River drainage system also reveal almost no areas along the present-day channels where sediment could be stored for significant quantities of time. There is, however, a possibility that a small fraction of the finer-grained sediment components could be aeolian in origin, in which case a sample's comminution age could be significantly older than its depositional age.

4. Methods

In order to obtain the ($^{234}U/^{238}U$) activity ratio of the detrital component as a function of grain size, the following five steps were performed on the raw samples identified in Figure 3b: 1) sequential leaching to remove nondetrital phases, modified from Tessier et al. (1979), 2) wet sieving and filtration using a Fritsch microsieve apparatus fitted with nylon sieve mesh and an Anopore filter, 3) dissolution of up to 100 mg of solid sample with a procedure employing HF, HNO_3, $HClO_4$, HCl, and H_3BO_3 acids, 4) column chemistry to isolate elemental U, modified from Luo et al. (1997), and 5) mass spectrometry to obtain high-precision U isotopic compositions, with measurements made using a Micromass Isoprobe multicollector inductively-coupled plasma mass spectrometer (MC-ICP-MS) (Christensen et al., 2004). Steps 3-5 follow conventional isotope geochemistry methods. Scanning electron microscopy (SEM) images showing a typical sample before and after both leaching and sieving (steps 1 and 2) are shown in Figure 4.

In addition to the U isotope measurements, Nd and Sr isotopes of the leached bulk (unsieved) samples were measured in order to determine sediment provenance, since the Sierra Nevada Batholith has a rough east-west gradient in Nd and Sr isotopes (Kistler, 1993). Further sample characterization was performed to obtain grain size distributions, measured using a Coulter particle analyzer, mineralogy by powder x-ray diffraction (XRD), and grain morphology and surface textures by scanning electron microscopy (SEM). Isotopic and grain size data are given in Table 1, and full methods are described in detail in Appendix A (Supplemental Information).

5. Results and discussion

5.1. Uranium isotope patterns

The uranium isotope results for sieved grain size separates and bulk samples (Figures 5 and 6a; Table 1) have many of the features expected if ^{234}U is lost from sediment grains primarily due to alpha recoil. All of the samples have ($^{234}U/^{238}U$) < 1 (secular equilibrium), indicating depletion of the ^{234}U daughter isotope. The comminution age model assumes that the grains' initial ($^{234}U/^{238}U$) = 1 for our nonporous parent material, and the high values of the youngest samples (0.9820 to 0.9978) suggest that this is a good assumption. The recoil model predicts larger ^{234}U depletions with increasing age, and the ($^{234}U/^{238}U$) values generally decrease with greater core depth for a given sieved size fraction (Figure 5). The deviation of the 21.34 m-depth sample from this age trend is discussed in Section 5.3.4.

Larger ^{234}U depletions are also expected as grain size decreases. Indeed, with the exception of the youngest sample, grains < 6 μm in diameter are more depleted in ^{234}U than the 10-20 μm grains, and the 10-20 μm grains are more depleted relative to the > 20 μm size fraction. Furthermore, the difference in ($^{234}U/^{238}U$) values between the < 6 μm fraction and the larger size fractions increases with age, as anticipated. The strong correlation between the ($^{234}U/^{238}U$) trends with depth for the unsieved and > 20 μm samples (Figure 6a) and the bulk grain size distributions (Figure 6b) also reflects the importance of grain size in controlling the magnitude of ^{234}U depletion.

The ($^{234}U/^{238}U$) activities are similar to those previously measured for fine-grained deep-sea sediments. The KRF sediments have ^{234}U depletions mostly in the range of 1 - 8%, comparable to the 3 - 9% depletions observed for 0 - 400 ka North Atlantic drift sediments with short transport times and average grain sizes of 10-20 µm (DePaolo et al., 2006).

5.2. Glacial origin of sediments

The glacial origin and unweathered nature of the fine-grained KRF core sediment is supported by Nd and Sr isotope measurements for provenance and SEM images of grain surfaces. In the Kings River basin, the ranges of values for the Nd and Sr isotopic gradients across the Sierra Batholith, from west to east, are approximately from +6 to -7 ε_{Nd} units and from 0.704 to 0.709 for $^{87}Sr/^{86}Sr$ (Kistler, 1993). The isotopic values for the fine-grained channel and overbank deposits (Table 1) indicate that the provenance of most of the sediment is the plutonic rocks located in the eastern part of the range near the Sierran ridge crest, the high-elevation region most affected by Pleistocene glaciations. X-ray diffraction indicates a uniform granitic bulk mineralogy for the fine-grained sediments. SEM images of grain surfaces reveal features indicating glacial abrasion and limited subaerial weathering (angular shapes, fresh breakage surfaces, step fractures, chattermarks, and parallel gouges & striations) (e.g., Sharp and Gomez, 1986).

5.3. Comminution age calculations and behavior of f_α

5.3.1. Overview: Evaluating the accuracy of the comminution ages

After obtaining the measured ($^{234}U/^{238}U$) values for the detrital fraction (Section 5.1), two variables remain unknown in the comminution age expression (Equation 1): the recoil loss factor f_α and the comminution age t_{comm}. The critical unknown parameter is f_α – if the appropriate f_α values can be determined, then it is possible to calculate comminution ages from the measured ($^{234}U/^{238}U$) values for samples where there are no independent constraints on the sediment age. Conversely, if the comminution ages are known, information about the behavior of the f_α value can be obtained. If both parameters are known, the accuracy of the comminution age method can therefore be evaluated by inputting one of the two variables into Eqn. 1, solving for the remaining parameter, and comparing the calculated value to the known value.

There are constraints on the f_α and t_{comm} values for the Kings River Fan core sediments, but the available information for both parameters is limited and carries significant uncertainty. Therefore, although the measured ($^{234}U/^{238}U$) values for the KRF sediments behave in a manner consistent with the recoil-based comminution age model – indicating that the method has the potential to successfully date terrestrial sediments – it is not possible to evaluate the accuracy of the method to high precision with the currently-available information.

In spite of the uncertainties in the f_α and t_{comm} values parameter values, Eqn. 1 can still be used to assess the first-order accuracy of the comminution ages, as well as elucidate trends in the behavior of f_α for the KRF sediments. In Sections 5.3.3 and 5.3.4, we present two sets of calculated comminution ages that utilize different approaches to estimating f_α. We show that even simple models for estimating f_α yield comminution ages that are plausible. The discrepancies between the literature-derived depositional ages and the calculated comminution ages suggest that 1) f_α is dependent on grain size, and 2) either f_α is age-dependent, or the KRF core sediments were deposited with a more constant deposition rate than indicated by the literature-derived age-depth model.

5.3.2. Describing f_α in terms of surface roughness

It is useful to discuss the recoil loss parameter f_α in terms of the surface roughness factor λ_r; this change of variables facilitates comparison with existing data describing sediment grain surfaces. The surface roughness factor (Helgeson et al., 1984; Jaycock and Parfitt, 1981; Anbeek et al., 1994) relates the smooth-surface geometric surface area to the actual surface area, which has 'roughness' (encompassing both small-lengthscale surface topography as well as internal grain surface area). As shown by DePaolo et al. (2006), f_α is generally much greater (10 - 50 times) than would be expected if the sediment grains were smooth spheres. The additional loss of ^{234}U implied by these elevated f_α values can be accounted for by the presence of grain surface roughness, which greatly increases the surface area over which recoil loss occurs. We can thus represent the recoil loss factor in terms of λ_r and the geometric grain size, which is well-constrained for our sieved size fractions, through the following equations:

$$f_\alpha = \frac{1}{4} L \cdot S_{tot} \cdot \rho \qquad (2)$$

(Semkow, 1990; DePaolo et al., 2006), where L is the recoil distance (34 nm; Sun and Semkow, 1998), ρ is the bulk density (assumed to be 2.65 x 10^6 g/m^3), and S_{tot} is given by the formulation of Anbeek et al. (1994) as:

$$S_{tot} = S_{geom} \cdot \lambda_r = (K/\rho d) \cdot \lambda_r \qquad (3)$$

where S_{geom} (m^2/g) is the geometric specific surface area, K is a dimensionless grain shape factor (Cartwright, 1962) equal to 6 for a sphere, and d is the grain diameter. f_α can then be related to the surface roughness by:

$$f_\alpha = \frac{LK}{4d} \lambda_r \qquad (4) .$$

Many studies where sediment surface areas are measured via gas adsorption techniques show that roughness is indeed significant, and grain surface areas have been estimated to be anywhere from several to hundreds of times larger than those calculated with a smooth sphere model (e.g., White and Peterson, 1990; Anbeek et al., 1994; Brantley and Mellott, 2000). For example, silicate samples freshly crushed or ground by mortar & pestle in the laboratory show relatively constant λ_r = 7 across a wide range of grain sizes (White and Peterson, 1990; Brantley and Mellott, 2000). However, studies of naturally-weathered samples suggest that λ_r increases with both increasing grain size (White and Peterson, 1990; Anbeek et al., 1994) and duration of subaerial weathering (White et al., 1996).

5.3.3. Calculating t_{comm} using a constant f_α value

A very simple approach for determining comminution ages from A_{meas} yields ages that are plausible, even on unsieved bulk samples. In this starting case, we calculate f_α for each sample from Eqn. 4, assuming all samples have common values of $\lambda_r = 7$, as suggested by previous studies, and $K = 6$. To determine d values, we use the grain size distributions (GSDs) measured by the Coulter analyzer to determine the grain diameter corresponding to the weighted average of the smooth-sphere specific surface area over the size range of interest. (For bulk samples, the size range is the full GSD; for the < 6 μm size fraction, the GSD is extrapolated down to 0.02 μm, the pore size of the wet-sieving filter). Comminution ages calculated with Eqn. 1 using A_{meas} and these f_α values are shown in Figure 7a. The ages for the bulk samples are within the range expected for these samples, and are similar to, although somewhat younger than, the literature values. This suggests that a straightforward first-order approach can provide useful information; e.g. the data indicate that the sediments are Late Quaternary in age and accumulated over a time period of ca. 500 kyr.

Surface roughness factors that vary as a function of grain size are, however, likely to be more appropriate than a constant value of $\lambda_r = 7$. In Figure 7a, the 10-15 μm and 15-20 μm size fractions require larger λ_r in order to agree with the literature ages, whereas the < 6 μm fraction requires smaller λ_r. Increasing λ_r with increasing grain size would also be consistent with previous studies of granitic sediment surface area (White and Peterson, 1990; Anbeek et al., 1994). Figure 7b shows the λ_r values required to match the measured ($^{234}U/^{238}U$) ratios to the literature-derived ages through Eqns. 1 and 4, and there are clear trends as a function of grain size. These trends indicate that, for natural samples, f_α is a more complicated function of grain size (and surface area) than previously suggested from considerations of grain geometry alone (e.g., Kigoshi, 1971). Although this analysis relies on the literature sediment ages, we find that using a simple linear age-depth curve instead of the literature ages (solid gray line in Figure 7a) produces relationships between λ_r and grain size that differ only slightly from those shown in Figure 7b. This reflects the high sensitivity of t_{comm} to f_α (and hence λ_r) values.

5.3.4. Calculating t_{comm} using f_α from the oldest samples

As an alternative to imposing independent estimates of λ_r, the measured ($^{234}U/^{238}U$) values for the oldest samples can be used to assess f_α because as the comminution age approaches 1 Ma, ($^{234}U/^{238}U$) values should approach a steady-state value of 1-f_α (cf. DePaolo et al., 2006). In addition to being the oldest sample, the sample at 43.80 m depth has the best independently-constrained age, since it is near the depth of the 780 ka Matuyama-Brunhes magnetic reversal at ~41 m. We use Eqn. 1 to calculate a set of f_α values corresponding to the bulk sample and size fractions of the 43.80 m sample, employing the literature-derived age of 820 ka and the measured ($^{234}U/^{238}U$). This set of f_α values is then applied to the younger samples to determine t_{comm}, thus taking into account the variation in f_α with grain size (discussed in terms of λ_r above). The comminution age-depth curve produced by this approach (Figure 8) resembles the curve for bulk samples with λ_r = 7 (Figure 7a), with ages that are plausible but younger than the literature age-depth curve.

There are two possible explanations for the younger-than-expected ages that we obtain using the comminution method. Although markedly less robust than the λ_r trend as a function of grain size, the first possibility is an unaccounted-for increase in λ_r (and hence f_α) as a function of age within the Turlock Lake Formation (colored data points in Figure 7b). This age dependence could be a weathering-induced effect, such as the increase in λ_r with age observed by White et al. (1996). An explanation for why the 21.34 m sample has larger-than-expected λ_r is suggested by the grain size distributions of the bulk samples – the distribution for the 21.34 m sample is markedly skewed towards finer grain sizes relative to the other samples (Figure 6b), although the bulk mineralogy as determined by XRD is essentially identical. This suggests that this sample was subjected to either different formation or sorting processes than the other samples, which may either generate or select for grains with different characteristic λ_r values. For example, if this sample was subjected to more vigorous glacial grinding that produced a larger population of small grains, this could have generated more roughness and porosity in the form of microcracks (Hodson, 1998). It is also possible that the 21.34 m sample is partly composed of older reworked sediment, which would lead to an apparent larger λ_r needed to relate A_{meas} to the literature age model.

A second possible explanation for the offset between the calculated comminution ages and the literature ages is that the middle part of the core could be younger than previously inferred. Although the correlations and age inferences discussed in Marchand and Allwardt (1981) and Lettis (1988) are quite reasonable, there are in fact no preexisting direct age determinations on the actual KRF sediments and only minimal paleomagnetic age constraints on KRF core B5. If the calculated comminution ages for the KRF core sediments (Figure 8) are the correct ages, then the age-depth model is roughly linear. A constant deposition rate is not wholly consistent with the accepted model for episodic fan deposition, but an age-depth model that is more linear than the current literature-derived model is not entirely implausible. This is because, as discussed in Section 3, there is uncertainty in the age of the Friant Pumice that constrains the age of the top of the Upper Turlock Lake Unit. In addition to these two possible explanations for the discrepancy between calculated comminution ages and literature ages, there may be potential complications with the comminution age method that we do not yet fully understand.

To summarize the findings discussed in Section 5.3 that are relevant to future applications of the comminution age method, deviations from expected comminution ages illuminate f_α trends with grain size and possibly age, which must be taken into account if the above approaches to calculating t_{comm} are used. To further improve the accuracy of the comminution age dating method, and to apply it to sediments that do not have independent age constraints, both 1) weathering effects and 2) perhaps more sophisticated approaches to determining f_α must be considered. These are discussed in Sections 5.4 and 5.5, respectively.

5.4. Effects of leaching and weathering

An argument for alpha recoil as the dominant process generating ^{234}U-^{238}U radioactive disequilibrium in the fine-grained Kings River Fan sediments is the similarity of literature λ_r values to those in Figure 7b, which were calculated assuming that recoil loss alone could account for the full magnitude of the measured (^{234}U/^{238}U) deficits. As a point of reference, λ_r values can exceed 600 (White et al. 1996). By comparison, the inferred surface roughness values of the KRF samples (approximately 1 to 17), are quite similar to values given for: 1) granitic glacial outwash (λ_r = ~0 to 8 for individual minerals < 20 μm diameter; Anbeek et al., 1994), 2) the youngest soil of the Merced chronosequence, which is composed of the same glacial outwash units from the Sierra Nevada as the nearby KRF sediments (λ_r = 21; White et al., 1996), and 3) fresh laboratory-ground silicates (λ_r = 7; White and Peterson, 1990; Brantley and Mellott, 2000). However, it is also possible that preferential leaching of ^{234}U, either naturally or during the sample pretreatment, has enhanced the apparent ^{234}U loss (Kolodny and Kaplan, 1970; Osmond and Ivanovich, 1992), since the λ_r values we calculate are somewhat larger than expected. This is based on comparison with the results of White et al. (1996) and Anbeek (1994), from which one would infer smaller values of λ_r in ≤ 20 μm samples. A strong argument against significant ^{234}U loss from preferential leaching, however, is that the youngest KRF samples (~200 ka) have very small depletions of ^{234}U of order 1%. Note also that previous studies of naturally-weathered samples have not explicitly dealt with small grains in the size ranges of our sieved samples, and extrapolating the λ_r trends from coarser samples may not be fully accurate.

One caveat in directly comparing literature λ_r values to those in Figure 7b is that the lengthscale of the measurement probe differs in these two cases. Surface areas are most commonly measured by BET gas adsorption. Since the characteristic lengthscale of alpha recoil (L = 34 nm) is two orders of magnitude greater than the length of the BET adsorbate molecules (typically N_2, with a diameter of ~ 0.35 nm), the S_{tot} surface areas obtained by the two methods can only be directly compared if the roughness of the surface is greater than or equal to the recoil lengthscale. This may be likely, since most natural minerals at the Earth's surface are dominantly mesoporous (Rama and Moore, 1984; Brantley and Mellott 2000, and refs. therein), where mesoporous is defined as having a characteristic porosity (roughness) lengthscale of 2-50 nm. If there is substantial microporosity (< 2 nm), BET-determined values of λ_r from the literature will yield values that are larger than recoil-based λ_r.

When surface roughness is parameterized in terms of fractal dimension (D), a similarity between literature D values and those for the KRF sediments also is revealed. For surfaces, values for D typically range from $2 \leq D < 3$, where 2 corresponds to Euclidean geometry (i.e., no surface roughness) and 3 corresponds to an infinitely rough surface. The recoil loss factor f_α is related to D by the following scaling relationship from Semkow (1991):

$$f_\alpha \propto d^{(D-3)} \qquad (5)$$

Therefore, on a plot of log f_α vs. log d, the slope of a line will be equal to (D-3). We obtain the fractal dimension by first using A_{meas} and literature ages to calculate f_α values for the KRF sieved size fractions, then plotting against the grain diameter d values. A linear least-squares regression yields the following fractal dimensions for the Turlock Lake Formation samples: for samples at depths of 12.59, 21.34, 31.24, and 43.80 m, the corresponding fractal dimensions are 2.58 ± 0.12, 2.82 ± 0.01, 2.65 ± 0.05, and 2.50 ± 0.12, respectively, where uncertainties are standard errors on the regression slope. We are unable to determine a meaningful D for the 3.81 m Riverbank Formation sample because the <6 μm fraction is not the most depleted size fraction. These relatively high D values for the other KRF samples are similar to the range of D values obtained by both molecular tiling and radon emanation methods for other rocks and soils (Avnir et al., 1984; Avnir et al., 1985; Semkow, 1991), lending further support to the idea that alpha recoil can fully account for the magnitude of ($^{234}U/^{238}U$) depletion. It should be noted that an advantage of using this Rn emanation method of Semkow (1991) to get D is that the resulting fractal dimensions are relevant for describing self-similarity on the lengthscale of recoil (tens of nm).

In addition to preferential leaching of ^{234}U, other complicating factors from weathering can affect the U isotopic composition of sediment grains. The simplest model of weathering is the progressive dissolution and removal of the grains' surface layer, which reduces the diameter and partially removes the outer rinds depleted in ^{234}U by the recoil process. In this model, if weathering occurs at a fast enough rate (DePaolo et al., 2006), the magnitude of the ^{234}U depletion would be limited, thereby skewing the comminution ages to lower values. Weathering rates have been studied extensively for developed soils, but data are scarce for sediments that are barely subjected to soil-forming processes, as is the case for most of the KRF samples we analyzed. One study that does investigate such sediments is Maher et al. (2003). In this study, the deduced bulk weathering rate for the 15 – 700 ka granitic sediments of the Hanford Formation in south-central Washington State is 3 x 10^{-17} mol/m^2/sec when referenced to the smooth-sphere model surface area of the sediments. However, considering that the grains' surface area is roughly ten times the smooth-sphere area, this rate corresponds to a timescale of roughly 3500 kya to dissolve a surface layer of thickness equal to the recoil distance of 34 nm. The dissolution timescale is therefore about ten times the timescale for ^{234}U depletion by recoil, so weathering may not significantly retard the growth of ^{234}U depletion effects.

It is also possible that weathering can promote ^{234}U depletion if the dominant weathering effect is an increase in surface roughness rather than dissolution and removal of ^{234}U-depleted grain surface regions. Enhanced ^{234}U recoil loss with sample aging could explain the young comminution ages obtained when f_{α} is estimated from the oldest sample (Section 5.3.4). Excess recoil loss would be facilitated if the dissolution process that generates increased roughness only partially samples the ^{234}U-depleted regions. This would be the case if mineral dissolution occurs mainly from pore bottoms, which comprise a small proportion of the total surface area (Anbeek et al., 1994).

The coarse-grained, moderately mature paleosol sample at 8.38 m depth (Table 1) provides some indication about the possible effects of long-term and/or intense subaerial weathering. This sample shows anomalous behavior when compared to the glacial flour samples – values of ($^{234}U/^{238}U$) decrease with increasing grain size, and all ($^{234}U/^{238}U$) values are greater than the secular equilibrium value. The grain size trend may be explained by factors that are correlated with available surface area, given the decreasing surface area to volume ratio as grain size increases. Possible factors include the presence of secondary grain coatings with high U concentrations and/or high ($^{234}U/^{238}U$) (e.g., Plater et al., 1992) which may provide a source for implanted ^{234}U, or be incompletely removed during the sequential leaching sample pretreatment. In addition to the high-^{234}U nondetrital phases directly targeted by the sequential leaching pretreatment (Table A1), secondary phases formed by weathering can preferentially concentrate ^{234}U (e.g., Pelt et al., 2008), particularly illite and montmorillonite (Shirvington, 1983).

5.5. Additional means of independently determining f_α

In addition to the approaches discussed in Section 5.3, several other methods may be used to independently determine the value of the f_α parameter needed to calculate t_{comm} from the measured ($^{234}U/^{238}U$) values using Eqn. 1 (Table 2). An advantage of the methods discussed in this section is that f_α may be directly determined for each individual sample. This may lead to more precise and accurate comminution ages for a given sample.

One approach is to measure ($^{226}Ra/^{230}Th$) activity ratios on the same samples for which the ($^{234}U/^{238}U$) values are determined (DePaolo et al., 2006). Compared to the ^{238}U-^{234}U parent-daughter pair, the alpha recoil decay of ^{230}Th to ^{226}Ra – also in the ^{238}U decay chain – has a similar recoil distance but a much shorter half life of only 1599 yrs. Therefore, the ($^{230}Th/^{226}Ra$)

value will reach the 1-f_α steady state value relatively quickly (within ~10 ka). For samples older than ~10 ka, the f_α value determined from the steady-state value of ^{230}Th-^{226}Ra can then be applied to the ^{238}U-^{234}U system, with a minor correction for the slight difference in recoil distance for the different parent-daughter pairs (~37 nm recoil distance for the ^{230}Th decay (Sun and Semkow, 1998)). A small correction may also be needed to account for the recoil loss of some of the ^{234}U precursor to ^{230}Th.

Gas adsorption measurements can be used in several ways to determine f_α. The first way is to measure the grain surface area over which alpha recoil occurs, allowing f_α to be calculated using Eqn. 2. As discussed in Section 5.4, the 'yardstick' for obtaining surface areas via the commonly-used BET model for gas adsorption is the lengthscale associated with the adsorbate molecule. Therefore, BET surface areas can provide a direct measurement of the surface area over which recoil occurs only if the lengthscale of the sample surface roughness is roughly equal to or greater than the recoil lengthscale (i.e., mesoporous and macroporous solids, with minimal microporosity that can contribute additional superfluous surface area). If BET surface areas are used to calculate f_α, the accompanying full adsorption/desorption isotherm should also be measured to characterize the pore size distribution of the sample.

Another way of using gas adsorption measurements to determine f_α is to employ a grain surface area model that relates the angstrom-scale surface structures probed by BET analysis to the larger recoil-lengthscale roughness. One such model is that of Semkow (1990), which describes the surface from which recoiled daughters are ejected as having fractal geometry. To obtain f_α, the following relation may be used (Semkow, 1990; Bourdon et al., 2009):

$$f_\alpha = \frac{1}{4}\left[\frac{2^{D-1}}{4-D}\left(\frac{a}{L}\right)^{D-2}\right] L \cdot S_{BET} \cdot \rho \qquad (6)$$

where S_{BET} is the measured BET surface area and a is the adsorbate molecule diameter (0.35 nm for N_2). The fractal dimension D must be determined independently, which can also be done with gas adsorption measurements.

There are three approaches for obtaining fractal dimensions at recoil lengthscales (Jaroniec, 1995; Lowell et al., 2004), which are comparable to mesoporosity lengthscales. The first is through the use of the Frenkel-Halsey-Hill (FHH) adsorption isotherm equation (Avnir and Jaroniec, 1989; Yin, 1991). The FHH relation states that $N \propto [\ln(P_0/P)]^{D-3}$, where N is the amount of adsorbed gas at the relative pressure P/P_0, P is the equilibrium gas pressure, and P_0 is the saturation pressure. Therefore, on a plot of ln N vs. ln(ln(P/P_0), the fractal dimension can be obtained from the slope of (D – 3). This relation holds for relative pressures in the capillary (pore) condensation regime. The second approach is the Neimark-Kiselev (NK) thermodynamic method (Neimark, 1990; Neimark 1992), in which the characteristic lengthscale of the measurement 'yardstick' is a_c, the mean radius of meniscus curvature for the condensed adsorbate within a pore. In the NK model, $S_{\mathrm{lg}} = K{a_c}^{2-D}$. Here K is a constant, the adsorbate-vapor (liquid-gas) interfacial area S_{lg} can be calculated using the Kiselev equation, and a_c is related to the relative pressure through the Kelvin equation (Neimark, 1990). The third method for obtaining D is through the slope of a log-log plot of the pore size distribution $J(r)$, where r is the average pore radius (Jaroniec, 1995): $J(r) \propto r^{2-D}$. Previous studies indicate that the FHH and NK methods can be equivalent (Jaroniec, 1995; Sahouli et al., 1996).

6. Conclusions

To investigate whether continental sediments can be dated to useful accuracy with the uranium-series comminution age method, we applied the method to the glacigenic alluvial deposits of the Kings River Fan. Samples were obtained from a 45 meter-long drill core that contains minimally-weathered sediment deposited since ~800 kya. Independent age estimates on the sediments are available, although they are based on stratigraphic correlations to other alluvial fan sections north of our sampling site. The glacial origin of the sediments was verified using Nd and Sr isotopes, as well as SEM imaging. Precise U isotopic measurements were made on bulk sediment and sieved grain size fractions, all of which were first sequentially leached to remove nondetrital phases.

Based on our results, the U-series comminution age method appears to have promise for dating continental sediments, although there is need for considerable further work. The U isotope ratios for the KRF samples behave in a manner consistent with the comminution age model, where ^{234}U loss primarily occurs due to alpha recoil. The (^{234}U/^{238}U) activity ratios of bulk sediment samples, as well as the > 20 μm, 15-20 μm, 10-15 μm, and < 6μm fractions, have ^{234}U depletions of up to 9% (relative to secular equilibrium) that generally increase down core. The (^{234}U/^{238}U) values also depend on grain size: the smallest grains < 6 μm in diameter are more depleted in ^{234}U than the larger 10-20 μm grains, and the 10-20 μm grains are more depleted relative to the > 20 μm size fraction.

The deduced ages for the KRF samples are plausible even for relatively crude approaches to the data interpretation. Calculated comminution ages are obtained by using two simple approaches to determining the recoil loss parameter f_α: 1) using a constant value of λ_r, and 2) applying f_α values derived from the (^{234}U/^{238}U) values from the oldest KRF samples. The age estimates we derive for KRF sediments using these approaches are 50 to 100 kya at the top of the 45 meter section and 500 to 800 kya at the bottom. For comparison, the available age and correlation analysis from the literature suggests that the sediment ages are between 200 and 800 ka. Deviations from the literature-derived age-depth model for the grain size separates suggest that λ_r increases with increasing grain size and possibly age. The ranges of values for λ_r (1 to 17) and the fractal dimension D (2.50 to 2.82) are consistent with alpha recoil loss of ^{234}U being the main cause of ^{234}U depletions in the sediments.

Further work is needed in order to determine the role of weathering (including the processes of mineral dissolution and aqueous leaching of ^{234}U) in affecting the (^{234}U/^{238}U) values of the detrital sediment fraction. ^{238}U-^{234}U-^{230}Th disequilibrium may be useful for investigating these weathering processes. The anomalous behavior of a moderately mature paleosol sample indicates that intensely weathered samples may have (^{234}U/^{238}U) values that reflect the U concentration and isotopic composition of nondetrital grain coatings.

A priority for future work is to obtain more precise values for f_α on individual samples. Among the ways this can be done is through the measurement of (^{226}Ra/^{230}Th) activities, as well as gas adsorption measurements to characterize the sample surface area. A fractal model for surface roughness can be used to translate BET surface areas into the relevant surface area for recoil loss of ^{234}U; creating other models for surface roughness may also be useful.

Acknowledgements

We thank Shaun Brown, Evan Kha, Tom Owens, and Tim Teague for laboratory and technical assistance. Graham Fogg (UC Davis) granted access to samples from KRF core B5, and Bill Dietrich provided comments and allowed us the use of the Coulter particle sizer. We are also grateful for comments from two anonymous reviewers. Funding for this project was provided by National Science Foundation (NSF) grant EAR-0617744, Lawrence Livermore National Laboratory UEPP, and an NSF Graduate Research Fellowship to V.Lee. The work was also facilitated by support from the Department of Energy Office of Basic Energy Sciences under contract DE-AC02-05CH11231 to Lawrence Berkeley National Laboratory.

References

Aitken, M.J., 1998. An Introduction to Optical Dating: The Dating of Quaternary Sediments by the Use of Photon-stimulated Luminescence, Oxford University Press, Oxford, UK, 267 pp.

Anbeek, C., Vanbreemen, N., Meijer, E.L., Vanderplas, L., 1994. The Dissolution of Naturally Weathered Feldspar and Quartz. Geochim. Cosmochim. Acta 58 (21), 4601-4613.

Avnir, D., Farin, D., Pfeifer, P., 1984. Molecular Fractal Surfaces. Nature 308 (5956), 261-263.

Avnir, D., Farin, D., Pfeifer, P., 1985. Surface Geometric Irregularity of Particulate Materials - the Fractal Approach. J. Colloid Interface Sci. 103 (1), 112-123.

Avnir, D., Jaroniec, M., 1989. An Isotherm Equation for Adsorption on Fractal Surfaces of Heterogeneous Porous Materials. Langmuir 5 (6), 1431-1433.

Brantley, S.L., Mellott, N.P., 2000. Surface area and porosity of primary silicate minerals. Am. Mineral. 85 (11-12), 1767-1783.

Burow, K., Panshin, S.Y., Dubrovsky, N.M., Van Brocklin, D., Fogg, G.E., Evaluation of processes affecting 1,2-Dibromo-3-Chloropropane (DBCP) concentrations in ground water in the eastern San Joaquin Valley, California: Analysis of chemical data and ground-water flow and transport simulations, Water-Resources Investigations, U.S. Geological Survey, 1999, p. 57.

Cartwright, J., 1962. Particle Shape Factors. Ann. Occup. Hyg. 5 163-171.

Chabaux, F., Riotte, J., Dequincey, O., 2003. U-Th-Ra fractionation during weathering and river transport. Uranium-Series Geochemistry 52, 533-576.

Christensen, J.N., Dresel, P.E., Conrad, M.E., Maher, K., Depaolo, D.J., 2004. Identifying the sources of subsurface contamination at the Hanford Site in Washington using high-precision uranium isotopic measurements. Environ. Sci. Technol. 38 (12), 3330-3337.

DePaolo, D.J., Maher, K., Christensen, J.N., McManus, J., 2006. Sediment transport time measured with U-series isotopes: Results from ODP North Atlantic drift site 984. Earth Planet. Sci. Lett. 248 (1-2), 394-410.

Dietrich, W.E., Dunne, T., Humphrey, N.F., Reid, L.M., 1982. Construction of sediment budgets for drainage basins, in: Swanson, F.J., Janda, R.J., Dunne, T., Swanston, D.N., (Eds), U.S.D.A. Forest Service General Technical Report PNW-141, Pacific Northwest Forest and Range Experiment Station, Portland, Oregon, pp. 5-23.

Dietrich, W.E., Bellugi, D., Heimsath, A.M., Roering, J.J., Sklar, L., Stock, J.D., 2003. Geomorphic transport laws for predicting the form and evolution of landscapes. In: Wilcock, P., Iverson, R., (Eds), Prediction in Geomorphology, AGU Geophysical Monograph Series 135, pp. 103-132.

Dosseto, A., Bourdon, B., Turner, S.P., 2008. Uranium-series isotopes in river materials: Insights into the timescales of erosion and sediment transport. Earth Planet. Sci. Lett. 265 (1-2), 1-17.

Dunne, T., Mertes, L.A.K., Meade, R.H., Richey, J.E., Forsberg, B.R., 1998. Exchanges of sediment between the flood plain and channel of the Amazon River in Brazil. Geol. Soc. Am. Bull. 110 (4), 450-467.

Gosse, J.C., Phillips, F.M., 2001. Terrestrial in situ cosmogenic nuclides: theory and application. Quat. Sci. Rev. 20 (14), 1475-1560.

Granet, M., Chabaux, F., Stille, P., France-Lanord, C., Pelt, E., 2007. Time-scales of sedimentary transfer and weathering processes from U-series nuclides: Clues from the Himalayan rivers. Earth Planet. Sci. Lett. 261 (3-4), 389-406.

Hashimoto, T., Aoyagi, Y., Kudo, H., Sotobayashi, T., 1985. Range Calculation of Alpha-Recoil Atoms in Some Minerals Using Lss-Theory. J. Radioanal. Nucl. Chem. 90 (2), 415-438.

Hay, W.W., 1998. Detrital sediment fluxes from continents to oceans. Chem. Geol. 145 (3-4), 287-323.

Helgeson, H.C., Murphy, W.M., Aagaard, P., 1984. Thermodynamic and kinetic constraints on reaction rates among minerals and aqueous solutions. II. Rate constants, effective surface area, and the hydrolysis of feldspar. Geochim. Cosmochim. Acta 48 (12), 2405-2432.

Hodson, M.E., 1998. Micropore surface area variation with grain size in unweathered alkali feldspars: implications for surface roughness and dissolution studies. Geochim. Cosmochim. Acta 62 (21-22), 3429-3435.

Huntington, G.L., 1980. Soil-Land Form Relationships of Portions of the San Joaquin River and Kings River Alluvial Depositional Systems in the Great Valley of California, Ph.D., University of California at Davis.

Janda, R.J., 1966. Pleistocene history and hydrology of the upper San Joaquin River, California, Ph.D., University of California, Berkeley.

Jaroniec, M., 1995. Evaluation of the Fractal Dimension from a Single Adsorption-Isotherm. Langmuir 11 (6), 2316-2317.

Jaycock, M.J., Parfitt, G.D., 1981. Chemistry of Interfaces, Ellis Horwood.

Kigoshi, K., 1971. Alpha-Recoil Thorium-234: Dissolution into Water and Uranium-234/Uranium-238 Disequilibrium in Nature. Science 173 (3991), 47-48.

Kistler, R.W., 1993. Mesozoic Intrabatholithic Faulting, Sierra Nevada, California. In: Dunn, G.C., McDougall, K.A., (Eds), Mesozoic Paleogeography of the Western United States -

II 71, Pacific Section, Society of Economic Paleontologists and Mineralogists, Los Angeles, pp. 274-262.

Kolodny, Y., Kaplan, I.R., 1970. Uranium Isotopes in Sea-Floor Phosphorites. Geochim. Cosmochim. Acta 34 (1), 3-24.

Last, W.M., Smol, J.P., 2001. Tracking Environmental Change Using Lake Sediments, Klewer Academic Publishers, Dordrecht.

Lettis, W.R., 1988. Quaternary Geology of the Northern San Joaquin Valley. In: Graham, S.A., (Ed), Studies of the Geology of the San Joaquin Basin 60, Pacific Section S.E.P.M., pp. 333-351.

Lowell, S., Shields, J.E., Thomas, M.A., Thommes, M., 2004. Characterization of Porous Solids and Powders: Surface Area, Pore Size and Density, Kluwer Academic Publishers, Dordrecht, The Netherlands, 347 pp.

Luo, X.Z., Rehkamper, M., Lee, D.C., Halliday, A.N., 1997. High precision Th-230/Th-232 and U-234/U-238 measurements using energy-filtered ICP magnetic sector multiple collector mass spectrometry. Int. J. Mass Spectrom. 171 (1-3), 105-117.

Maher, K., DePaolo, D.J., Conrad, M.E., Serne, R.J., 2003. Vadose zone infiltration rate at Hanford, Washington, inferred from Sr isotope measurements. Water Resour. Res. 39 (8), 1204.

Maher, K., DePaolo, D.J., Christensen, J.N, 2006, U-Sr Isotopic Speedometer: Fluid flow and Chemical Weathering Rates in Aquifers. *Geochimica et Cosmochimica Acta*, v. 70, 4417-4435.

Marchand, D.E., 1977. The Cenozoic history of the San Joaquin Valley and the adjacent Sierra Nevada as inferred from the geology and soils of the eastern San Joaquin Valley. In:

Singer, M.J., (Ed), Soil Development, Geomorphology, and Cenozoic History of the Northeastern San Joaquin Valley and Adjacent Areas, California. Guidebook for Joint Field Session, Soil Science Society of America and Geological Society of America, University of California Press, pp. 39-50.

Marchand, D.E., Allwardt, A., 1981. Late Cenozoic Stratigraphic Units, Northeastern San Joaquin Valley, California, U.S. Geological Survey Bulletin 1470, United States Geological Survey Bulletin, p. 70.

Molnar, P., 2004. Late Cenozoic increase in accumulation rates of terrestrial sediment: How might climate change have affected erosion rates? Annu. Rev. Earth Planet. Sci. 32 67-89.

Neimark, A.V., 1990. Thermodynamic Method for Calculating Surface Fractal Dimension. JETP Lett. 51 (10), 607-610.

Neimark, A.V., 1992. A new approach to the determination of the surface fractal dimension of porous solids. Physica A 191 258-262.

Osmond, J.K., Ivanovich, M., 1992. Uranium-series mobilization and surface hydrology. In: Ivanovich, M., Harmon, R.S., (Eds), Uranium-series Disequilibrium: Applications to Earth, Marine, and Environmental Sciences, Clarendon Press, Oxford, pp. 259-288.

Pelt, E., Chabaux, F., Innocent, C., Navarre-Sitchler, A.K., Sak, P.B., Brantley, S.L., 2008. Uranium-thorium chronometry of weathering rinds: Rock alteration rate and paleo-isotopic record of weathering fluids. Earth Planet. Sci. Lett. 276 (1-2), 98-105.

Phillips, F.M., Zreda, M.G., Evenson, E.B., Hall, R.D., Chadwick, O.A., Sharma, P., 1997. Cosmogenic Cl-36 and Be-10 ages of Quaternary glacial and fluvial deposits of the Wind River Range, Wyoming. Geol. Soc. Am. Bull. 109 (11), 1453-1463.

Plater, A.J., Ivanovich, M., Dugdale, R.E., 1992. Uranium Series Disequilibrium in River Sediments and Waters - the Significance of Anomalous Activity Ratios. Appl. Geochem. 7 (2), 101-110.

Rama, Moore, W.S., 1984. Mechanism of Transport of U-Th Series Radioisotopes from Solids into Groundwater. Geochim. Cosmochim. Acta 48 (2), 395-399.

Raymo, M.E., Ruddiman, W.F., 1992. Tectonic Forcing of Late Cenozoic Climate. Nature 359 (6391), 117-122.

Sahouli, B., Blacher, S., Brouers, F., 1996. Fractal surface analysis by using nitrogen adsorption data: The case of the capillary condensation regime. Langmuir 12 (11), 2872-2874.

Sarna-Wojcicki, A.M., Pringle, M.S., Wijbrans, J., 2000. New Ar-40/Ar-39 age of the Bishop Tuff from multiple sites and sediment rate calibration for the Matuyama-Brunhes boundary. J. Geophys. Res.-Solid Earth 105 (B9), 21431-21443.

Semkow, T.M., Parekh, P.P., 1990. The Role of Radium Distribution and Porosity in Radon Emanation from Solids. Geophys. Res. Lett. 17 (6), 837-840.

Semkow, T.M., 1991. Fractal Model of Radon Emanation from Solids. Phys. Rev. Lett. 66 (23), 3012-3015.

Sharp, M., Gomez, B., 1986. Processes of Debris Comminution in the Glacial Environment and Implications for Quartz Sand-Grain Micromorphology. Sediment. Geol. 46 (1-2), 33-47.

Shirvington, P.J., 1983. Fixation of radionuclides in the 238U decay series in the vicinity of mineralized zones: 1. The Austatom Uranium Prospect, Northern Territory, Australia. Geochim. Cosmochim. Acta 47 (3), 403-412.

Sun, H.B., Semkow, T.M., 1998. Mobilization of thorium, radium and radon radionuclides in ground water by successive alpha-recoils. J. Hydrol. 205 (1-2), 126-136.

Syvitski, J.P.M., Peckham, S.D., Hilberman, R., Mulder, T., 2003. Predicting the terrestrial flux of sediment to the global ocean: a planetary perspective. Sediment. Geol. 162 (1-2), 5-24.

Tessier, A., Campbell, P.G.C., Bisson, M., 1979. Sequential Extraction Procedure for the Speciation of Particulate Trace-Metals. Anal. Chem. 51 (7), 844-851.

Vigier, N., Bourdon, B., Turner, S., Allegre, C.J., 2001. Erosion timescales derived from U-decay series measurements in rivers. Earth Planet. Sci. Lett. 193 (3-4), 549-563.

Wahrhaftig, C., Birman, J.H., 1965. The Quaternary of the Pacific Mountain System in California. In: Wright, H.E., Frey, D.G., (Eds), The Quaternary of the United States, A Review Volume for the VII Congress of the International Association for Quaternary Research., Princeton University Press, Princeton, NJ, pp. 299-340.

Weissmann, G.S., Mount, J.F., Fogg, G.E., 2002. Glacially driven cycles in accumulation space and sequence stratigraphy of a stream-dominated alluvial fan, San Joaquin valley, California, USA. J. Sediment. Res. 72 (2), 240-251.

Weissmann, G.S., Bennett, G.L., Lansdale, A.L., 2005. Factors controlling sequence development on Quaternary fluvial fans, San Joaquin Basin, California, USA. In: Harvey, A.M., Mather, A.E., Stokes, M., (Eds), Alluvial Fans: Geomorphology, Sedimentology, Dynamics 251, Geological Society of London, pp. 169-186.

White, A.F., Peterson, M.L., 1990. Role of Reactive-Surface-Area Characterization in Geochemical Kinetic Models. In, Chemical Modeling of Aqueous Systems II, American Chemical Society Symposium Series 416, pp. 461-475.

Yin, Y.B., 1991. Adsorption-Isotherm on Fractally Porous Materials. Langmuir 7 (2), 216-217.

Figure captions

Figure 1. Relationship of the uranium-series comminution age to other timescales of importance in sedimentary processes. The start of the comminution age "clock" is particularly well-defined for cases where the formation of fine-grained detrital clasts is rapid on a geologic timescale, such as during glacial comminution of bedrock. The utility of subdividing the comminution age is that these constituent timescales can also be determined from the comminution age, depending on the availability of additional information. The comminution age is equal to the depositional age in environments where the sediment transport + storage times are negligible. In settings where the depositional age is independently known, the comminution age is equal to the transport + storage time. Note that transport and storage of sediment particles can happen in multiple environments en route from formation to deposition (e.g., hillslope and fluvial environments in continental settings) – the transport + storage time includes the time spent in all of these environments.

Figure 2. Shaded relief map of the area of the Kings River Fan. Thick black line, outline of the Kings River drainage basin. Thin white line, outline of the glacially-derived Quaternary Kings River Fan alluvial deposits (after Weissmann et al., 2002). Star denotes the location of USGS sediment core B5, from which the samples in this study originate.

Figure 3. (a) Stratigraphic column of Kings River Fan core B5 showing depths of depositional units and facies. After Weissmann et al. (2002), reprinted with permission from SEPM (Society for Sedimentary Geology). **(b)** Age-depth relationship of the core sediments inferred from

previous studies (see text). The samples investigated in this study were five glacial flour samples (solid filled symbols) and one paleosol sample (× symbol).

Figure 4. (a) Scanning electron microscopy (SEM) image of sample KRF-70 prior to sample pretreatment. Note the large range of grain sizes and presence of nondetrital grain coatings. (**b)** SEM image of the sample KRF-70 after sequential leaching pretreatment and microsieving to isolate the 15 - 20 μm size fraction. This shows angular, unweathered, and minimally-damaged grains free of nondetrital coatings. The grains also occupy a narrow size range.

Figure 5. ($^{234}U/^{238}U$) activity ratios for sieved glacial flour samples (overbank and channel facies) with well-constrained upper and lower bounds on grain diameter. As expected from the comminution age model, these data show many characteristics consistent with having alpha recoil as the dominant mechanism for ^{234}U loss from the grains. These characteristics include ($^{234}U/^{238}U$) values < 1 that generally decrease with both age (depth) and grain size. The sample at 21.34 m depth departs from the age trend; this can be related to the sample's unique grain size distribution characteristics (see Section 5.4 text).

Figure 6. (a) ($^{234}U/^{238}U$) activity ratios for glacial flour samples with unconstrained bounds on upper and/or lower grain diameter. **(b)** Grain size distribution characteristics for bulk, unsieved glacial flour samples. D_{10}, D_{50}, and D_{90} denote the grain diameters at which 10%, 50%, and 90% of the sample particles have a smaller diameter, respectively. The U isotopic behavior is in accordance with the comminution age model and shows that the magnitude of the ^{234}U depletion is strongly influenced by grain size as well as age.

Figure 7. (a) Comminution ages calculated from the measured ($^{234}U/^{238}U$) values by assuming a constant surface roughness factor (λ_r) of 7 (symbols), as compared to the literature-derived age-depth model (solid line). This simple approach yields calculated comminution ages that are of the correct order of magnitude. However, grain size variations in λ_r are not accounted for, which is reflected in the scatter of calculated ages for different grain sizes at a given depth. **(b)** Surface roughness factors required for the measured ($^{234}U/^{238}U$) values to correspond to the literature model ages, as a function of grain diameter. Symbols correspond to those in Figure 3b. a, Riverbank Formation; b-e, Turlock Lake Formation. Calculations assume a shape factor of K = 6 and no internal surface area. λ_r is a clear function of grain size for the KRF sediments.

Figure 8. Comminution ages calculated using the measured ($^{234}U/^{238}U$) values and a set of f_α values derived from the 43.80 m sample (symbols), as compared to the literature-derived age-depth model (solid line). This approach does not take into account possible increases in f_α with age, which would shift the comminution ages for the younger samples to larger values, providing a better match to the literature age-depth curve.

Figure 1
Click here to download Figure: LeeEtal_Fig1.eps

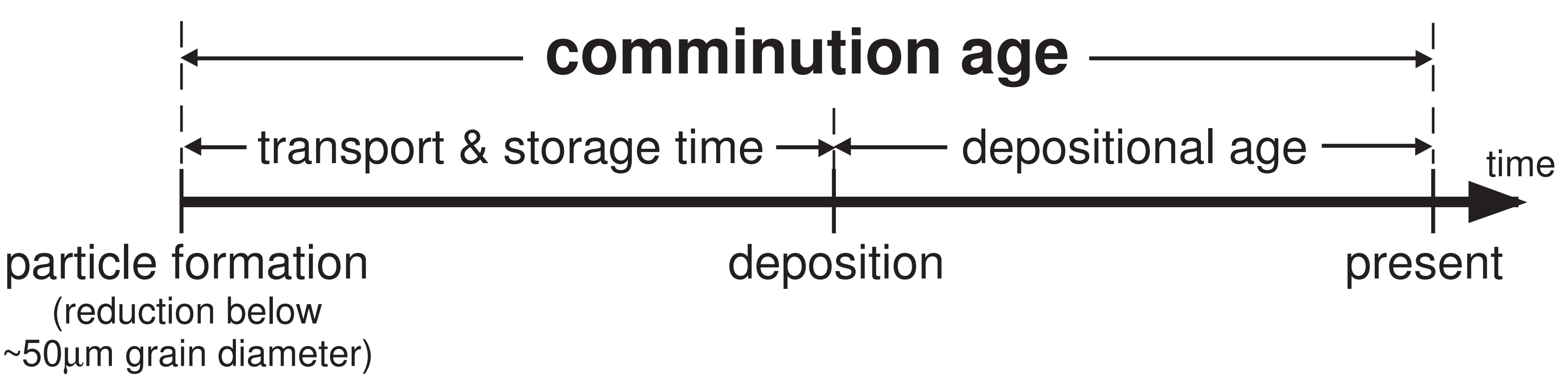

Figure 2
Click here to download Figure: LeeEtal_Fig2.eps

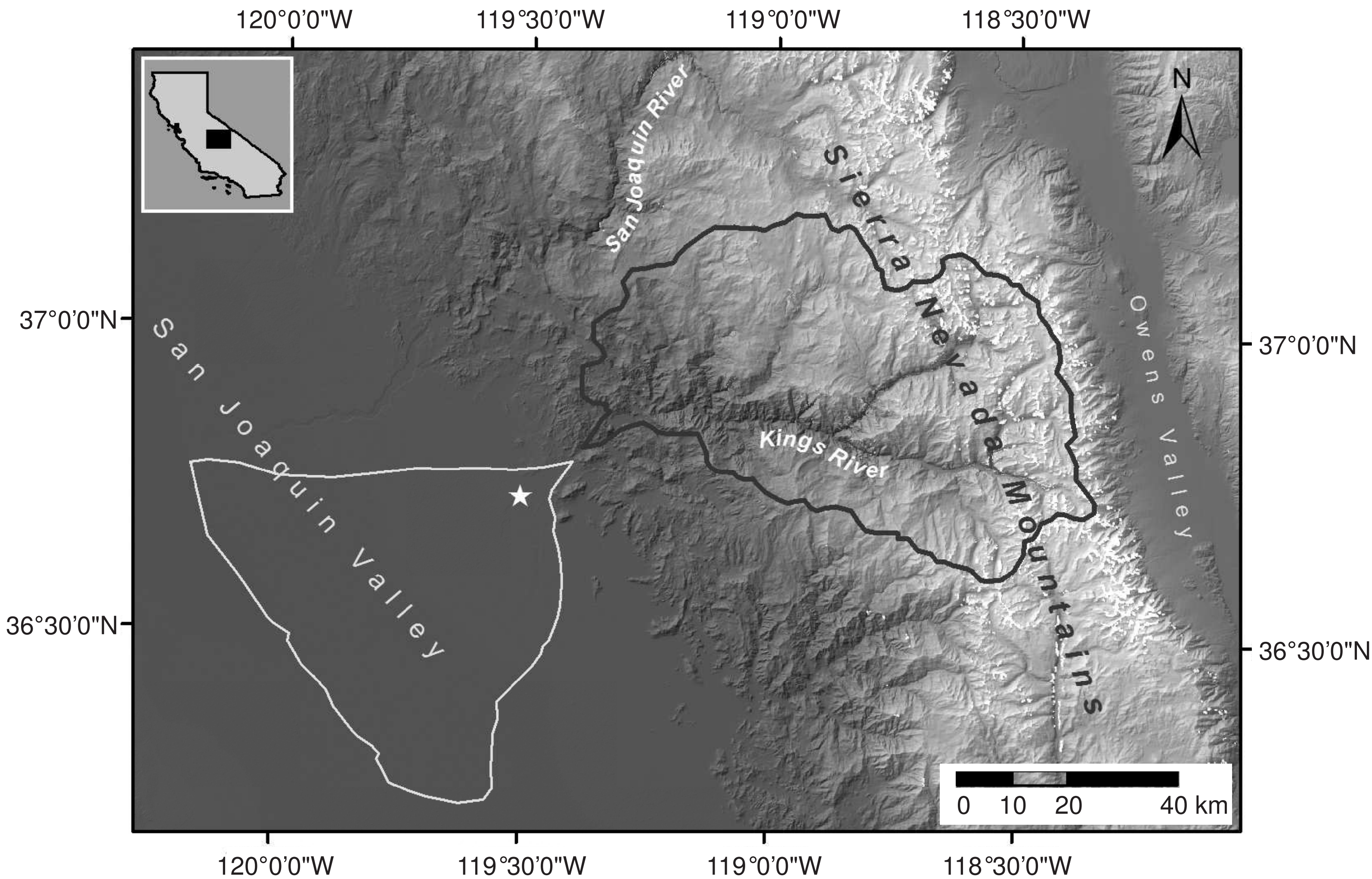

Figure 3

Click here to download Figure: LeeEtal_fig3.xls

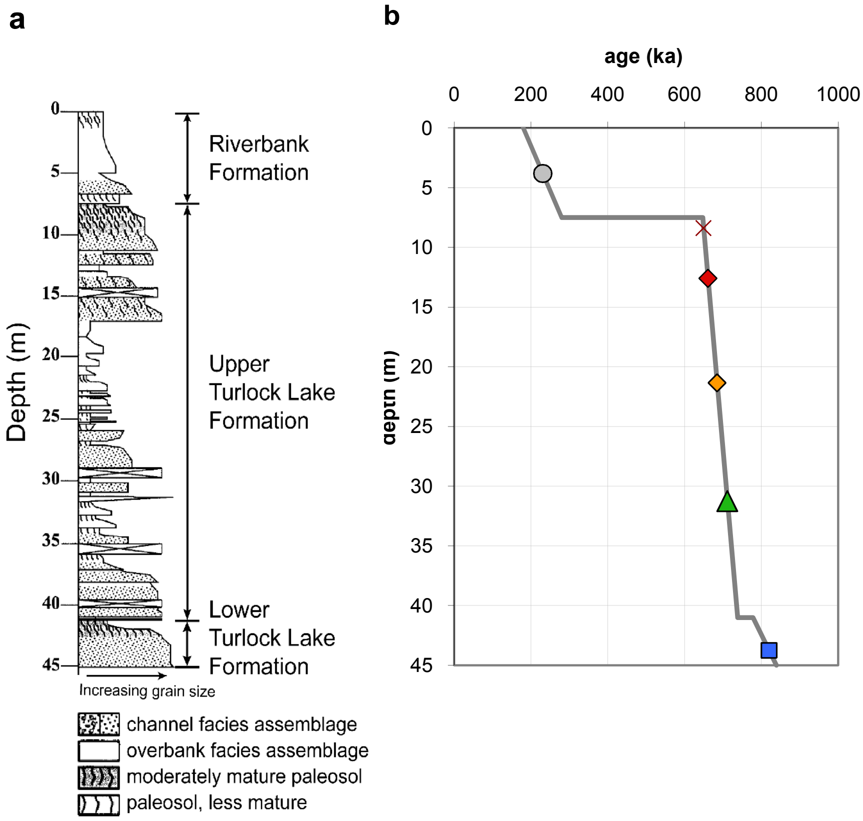

Figure 4
Click here to download high resolution image

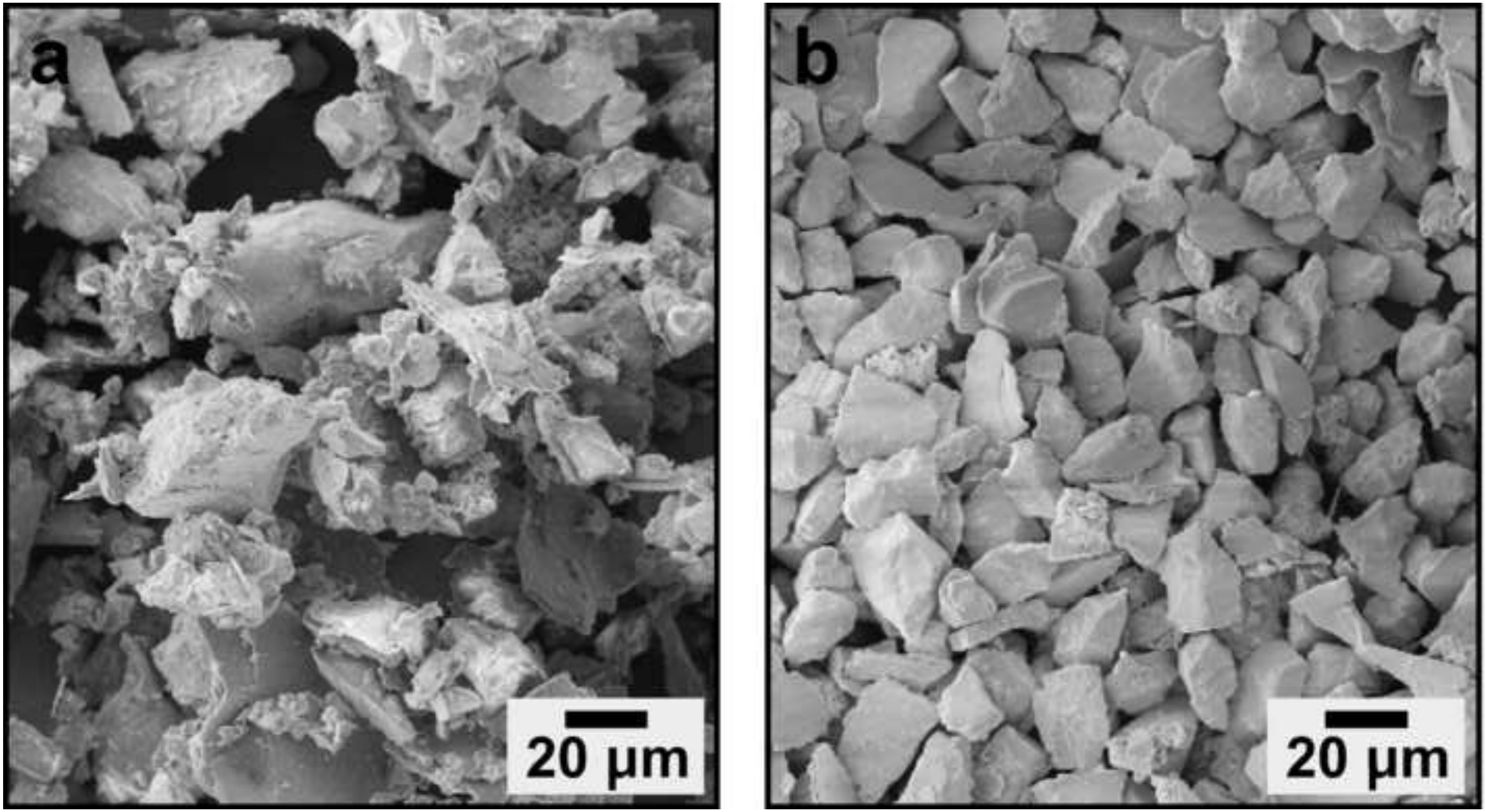

Figure 5

Click here to download Figure: LeeEtal_Fig5.xls

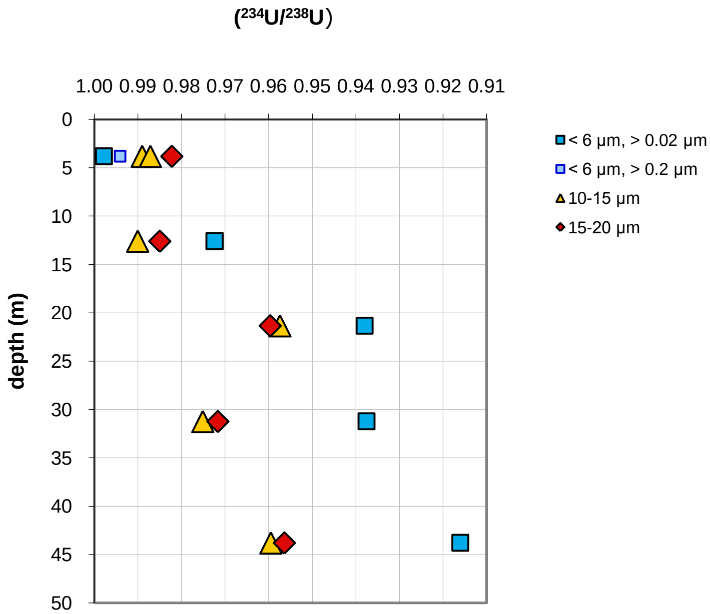

Figure 6

Click here to download Figure: LeeEtal_Fig6.xls

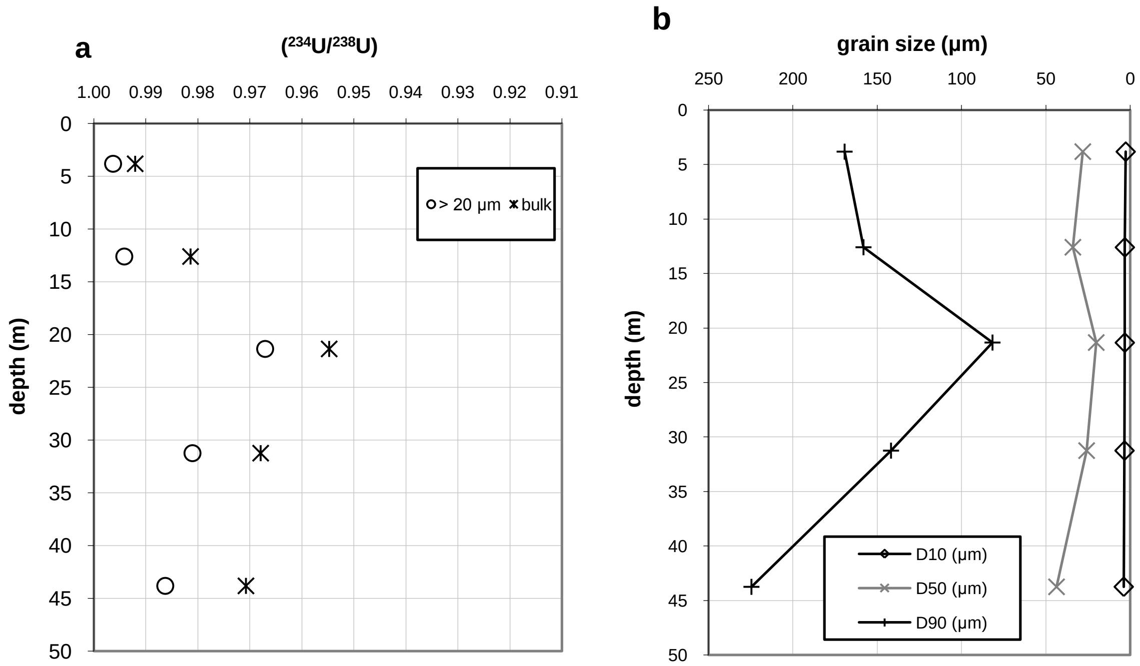

Figure 7

Click here to download Figure: LeeEtal_Fig7.xls

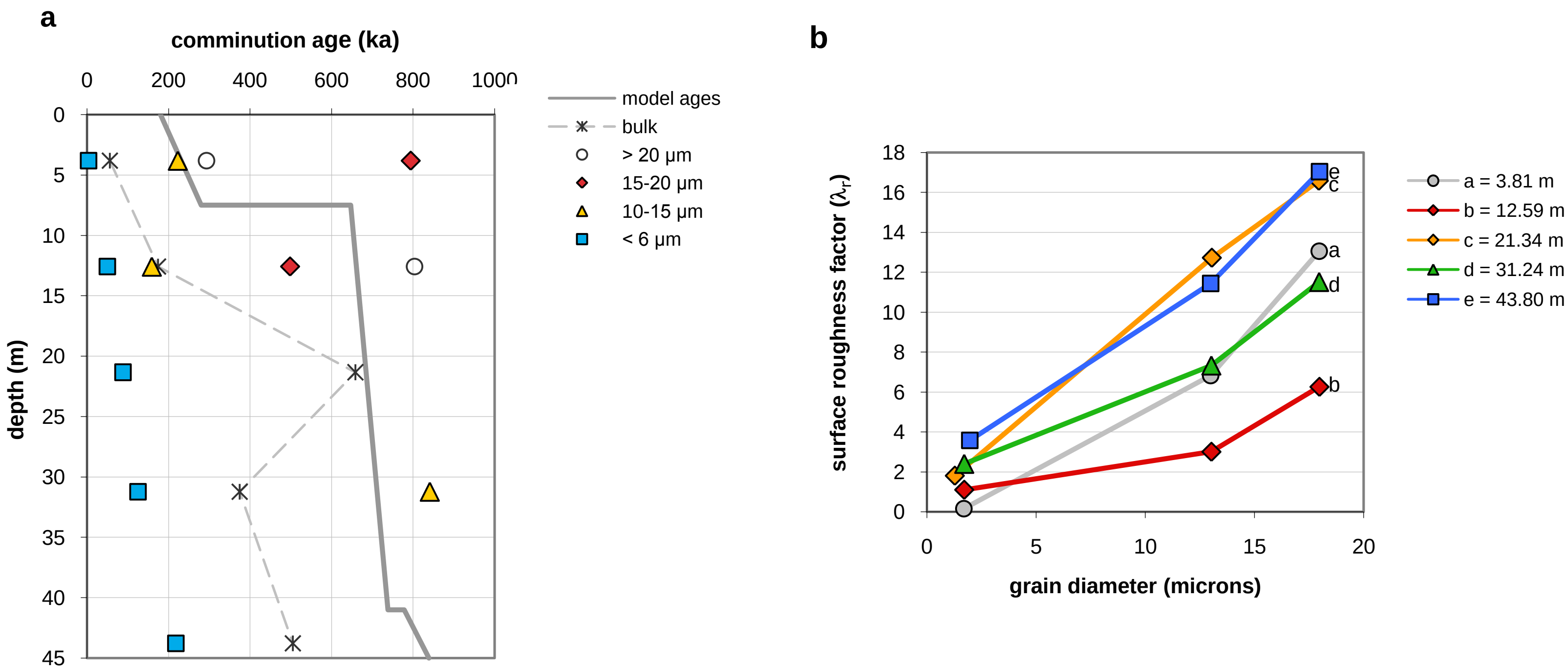

Figure 8

Click here to download Figure: LeeEtal_Fig8.xls

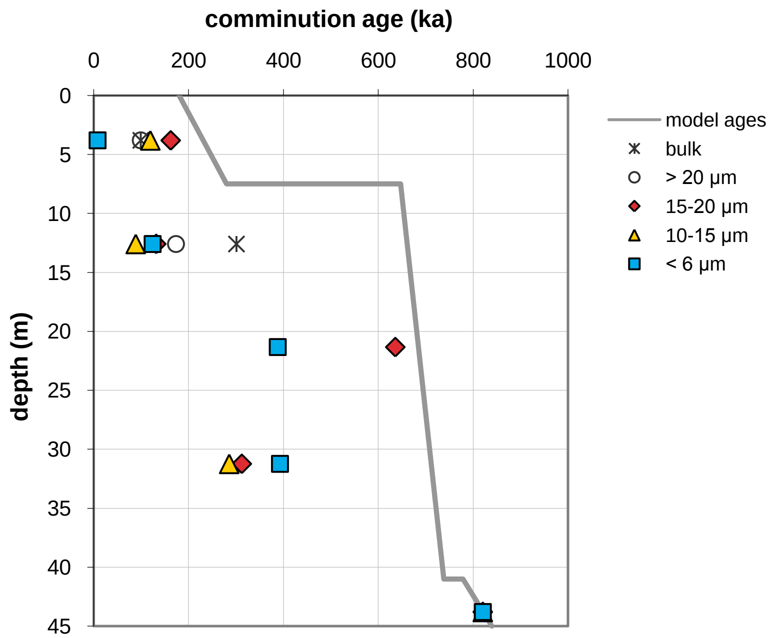

Table 1

TABLE 1. Kings River Fan core B5, isotopic and grain size analyses [a,b]

Depth (m)	Depositional facies	Depositional age[c] (ka)	D_{50} (µm)	ε_{Nd}	$^{87}Sr/^{86}Sr$	($^{234}U/^{238}U$) activity ratios[1]				
						Bulk sample	Grain diameters of sieved samples			
							> 20 µm	15-20 µm	10-15 µm	< 6 µm
3.81	overbank	230	28	-5.80 (10)	0.708132 (10)	0.9920 (29)	0.9963 (11)	0.9822 (12)	0.9872 (10)	0.9978 (12)
8.38	paleosol	650	201	+3.69 (10)	0.704803 (13)	1.0843 (32)	1.0310 (15)	--	1.1254 (39)	1.1569 (16)
12.59	overbank	660	34	-4.77 (12)	0.707914 (28)	0.9814 (28)	0.9941 (15)	0.9850 (13)	0.9901 (13)	0.9380 (10)
21.34	overbank	685	20	-5.10 (14)	0.708074 (13)	0.9547 (21)	0.9670 (15)	0.9597 (14)	0.9574 (17)	0.9724 (13)
31.24	overbank	710	26	-5.02 (14)	0.708167 (10)	0.9679 (30)	0.9810 (13)	0.9717 (12)	0.9751 (12)	0.9376 (11)
43.80	channel	820	44	-5.58 (14)	0.708364 (21)	0.9707 (15)	0.9863 (14)	0.9564 (16)	0.9595 (49)	0.9161 (14)

[a] Numbers in parentheses denote uncertainties in the last two digits of the reported value. Uncertainties on ($^{234}U/^{238}U$) values are 95% confidence intervals.
[b] D_{50}, Nd isotopes, and Sr isotopes are measured on bulk samples.
[c] Depositional age-depth model determined from Marchant & Allwardt (1981) and Lettis (1988).

Table 2

Click here to download Table: LeeEtal_Table2c.doc

TABLE 2. Summary of methods to determine the recoil loss factor f_α for ^{238}U-^{234}U decay

	Approach	Equation(s)		Comments
1)	Sieve samples to constrain grain diameter *d*, apply an appropriate surface roughness factor λ_r.	$f_\alpha = \frac{LK}{4d}\lambda_r$	(Eqn. 4)	λ_r may vary as a function of both grain size and sample age. λ_r must also describe surface roughness at the lengthscale of alpha recoil.
2)	Measure the ($^{234}U/^{238}U$) activity ratio of a sample old enough to be at steady state with respect to the ^{234}U and ^{238}U isotopes (> ~1 Ma) [a].	$f_\alpha = 1 - \left(\frac{^{234}U}{^{238}U}\right)$		Old samples may have f_α values that have increased with age, perhaps due to weathering.
3)	Measure the ($^{226}Ra/^{230}Th$) activity ratio from a sample at steady state with respect to the ^{230}Th and ^{226}Ra isotopes (> 10 ka) [a].	$f_\alpha = \left(\frac{34}{37}\right)\left[1 - \left(\frac{^{226}Ra}{^{230}Th}\right)\right]$		The (34/37) prefactor corrects for the slight difference in recoil distance for ^{234}U as compared to ^{230}Th.
4)	Directly obtain total surface area (S_{tot}) (e.g., measured from BET gas adsorption measurements).	$f_\alpha = \frac{1}{4}L \cdot S_{tot} \cdot \rho$	(Eqn. 2)	If S_{tot} is measured by BET gas adsorption, this approach is applicable only to solids with characteristic surface roughness lengthscales that are approximately equal to or greater than the alpha recoil distance (i.e., meso- and macro-porous solids).
5)	Obtain surface area from BET gas adsorption measurements (S_{BET}), translate to recoil-relevant lengthscales with a model for surface roughness. Example: fractal model for surface roughness [b].	$f_\alpha = \frac{1}{4}\left[\frac{2^{D-1}}{4-D}\left(\frac{a}{L}\right)^{D-2}\right]L \cdot S_{BET} \cdot \rho$	(Eqn. 6)	Need to independently obtain fractal dimension *D* that describes roughness at the lengthscale of alpha recoil.
	Determining *D* from gas adsorption measurements [c]:			
	5a) Frenkel-Halsey-Hill	$N \propto [\ln(P_0/P)]^{D-3}$		
	5b) Neimark-Kiselev	$S_{lg} = Ka_c^{2-D}$		
	5c) Pore size distribution	$J(r) \propto r^{2-D}$		

[a] DePaolo et al., 2006
[b] Semkow, 1990
[c] Jaroniec, 1995; Lowell et al., 2004